

A Network Model of Catecholamine Effects: Gain, Signal-to-Noise Ratio, and Behavior

DAVID SERVAN-SCHREIBER, HARRY PRINTZ, JONATHAN D. COHEN

At the level of individual neurons, catecholamine release increases the responsiveness of cells to excitatory and inhibitory inputs. A model of catecholamine effects in a network of neural-like elements is presented, which shows that (i) changes in the responsiveness of individual elements do not affect their ability to detect a signal and ignore noise but (ii) the same changes in cell responsiveness in a network of such elements do improve the signal detection performance of the network as a whole. The second result is used in a computer simulation based on principles of parallel distributed processing to account for the effect of central nervous system stimulants on the signal detection performance of human subjects.

THE CATECHOLAMINES NOREPINEPHRINE and dopamine are neuroactive substances that are presumed to modulate information processing in the brain rather than to convey discrete sensory or motor signals. Release of norepinephrine and dopamine occurs over wide areas of the central nervous system (CNS), and the postsynaptic effects of the release of these catecholamines are long-lasting (1). One important effect consists of an enhancement of the response of target cells to other afferent inputs, inhibitory as well as excitatory [(2); reviewed in (3)].

Increases or decreases in catecholaminergic tone have many behavioral consequences, including effects on motivated behaviors, attention, learning, memory, and motor behavior. At the information processing level, catecholamines appear to affect the ability to detect a signal when it is embedded in noise [reviewed in (4)]. However, there is no adequate account of how these changes at the system level relate to the effect of catecholamines on individual cells. Several investigators (5–8) have suggested that catecholamine-mediated increases in a cell's responsiveness can be interpreted as a change in the cell's signal-to-noise ratio (SNR). By analogy, they proposed that this

change at the unit level may account for changes in signal detection performance at the behavioral level. We explore here the relation between these two levels, using mathematical and computational models of individual neurons and networks of neurons.

We assume that the response of a typical neuron can be described by a strictly increasing function $f_G(x)$ from real-valued inputs to the interval (0, 1). This function relates the strength of a neuron's net afferent input x to its probability of firing or activation. We do not require that f_G be differentiable or even continuous. We call f_G the activation function.

For instance, the family of logistics, given by

$$f_G(x) = \frac{1}{1 + e^{-(Gx+B)}} \quad (1)$$

has been proposed as a model of neural response functions (9). The logistics are all strictly increasing, for all values of $G > 0$ and all values of B .

The potentiating effect of catecholamines on responsiveness can be modeled as a change in the shape of the activation function. In the case of the logistic, this is achieved by increasing the value of the gain parameter G , as illustrated in Fig. 1B. As G increases, the value $f_G(x)$ comes arbitrarily close to 1 if $x > 0$ and arbitrarily close to 0 if $x < 0$ (10).

Consider the signal detection performance of a network in which the response of a single unit is compared with a threshold to determine the presence or absence of a signal. We assume that in the presence of the signal this unit receives a positive (excitatory) net afferent input x_s and in the absence of the signal it receives a null or negative

(inhibitory) input x_A . When zero-mean noise is added to this quantity, in the presence as well as in the absence of the signal, the unit's net input in each case is distributed around x_s or x_A , respectively (Fig. 1A). Therefore, its response is distributed around $f_G(x_s)$ or $f_G(x_A)$, respectively.

In other words, the input in the case where the signal is present is a random variable X_S , with probability density function (PDF) ρ_{X_S} , and in the absence of the signal it is the random variable X_A , with PDF ρ_{X_A} . These inputs then determine the random variables $Y_{GS} = f_G(X_S)$ and $Y_{GA} = f_G(X_A)$, with PDFs $\rho_{Y_{GS}}$ and $\rho_{Y_{GA}}$, which represent the response in the presence or absence of the signal for a given value of G (Fig. 1C).

If the input PDFs ρ_{X_S} and ρ_{X_A} overlap, the output PDFs $\rho_{Y_{GS}}$ and $\rho_{Y_{GA}}$ will also overlap. Thus, for any given threshold θ on the y axis

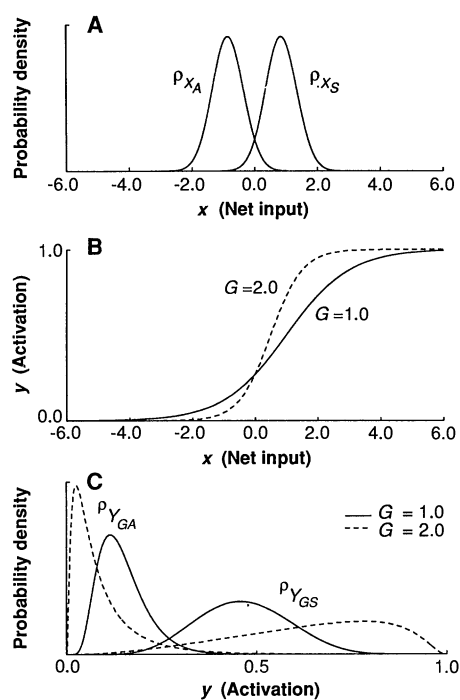


Fig. 1. (A) Example of the probability density function (PDF) of the net input in the cases of signal absent (ρ_{X_A}) and signal present (ρ_{X_S}). (B) The logistic function at two values of gain G . This function has been proposed as a model of neural responsiveness. The unit's activation at zero net input corresponds to a neuron's baseline firing rate. Positive net inputs correspond to excitatory stimuli, negative net inputs correspond to inhibitory stimuli. For the graphs drawn here, we set the bias B to -1 . The negative bias renders the function asymmetric around a net input of 0. This asymmetry is often found in the response function of actual neurons (22). Increasing G drives up a unit's response to a positive input and drives down its response to a negative input. (C) Examples of the PDFs of the activation value of a unit in the presence ($\rho_{Y_{GS}}$) and in the absence ($\rho_{Y_{GA}}$) of the signal. These are the PDFs of the transformed RVs, $Y_{GS} = f_G(X_S)$, and $Y_{GA} = f_G(X_A)$. Each PDF is drawn for two different values of G , in the case where f_G is the logistic.

D. Servan-Schreiber, School of Computer Science, Carnegie Mellon University, Pittsburgh, PA 15213 and Department of Psychiatry, School of Medicine, University of Pittsburgh, Pittsburgh, PA 15213.

H. Printz, School of Computer Science, Carnegie Mellon University, Pittsburgh, PA 15213 and Digital Equipment Corporation, Paris Research Laboratory, 85 Avenue Victor Hugo, 92563 Rueil-Malmaison Cedex, France.

J. D. Cohen, Department of Psychology, Carnegie Mellon University, Pittsburgh, PA 15213, Department of Psychiatry, School of Medicine, University of Pittsburgh, Pittsburgh, PA 15213, and Department of Psychiatry and Behavioral Sciences, School of Medicine, Stanford University, Stanford, CA 94305.

used to categorize the output as “signal present” or “signal absent,” there will be some misses and some false alarms. The best the system can do is to select a threshold that optimizes performance. More precisely, the expected payoff or performance of the unit is given by

$$E(\theta) = \lambda + \alpha \cdot \Pr(Y_{GS} \geq \theta) - \omega \cdot \Pr(Y_{GA} \geq \theta) \quad (2)$$

where λ , α , and ω are constants that together reflect the prior probability of the signal and the payoffs associated with correct detections (also called hits), correct ignores, false alarms, and misses. Note that $\Pr(Y_{GS} \geq \theta)$ and $\Pr(Y_{GA} \geq \theta)$ are the probabilities of a hit and a false alarm, respectively. By solving the equation $dE/d\theta = 0$, we can determine a threshold, θ^* , that maximizes E . We call θ^* the optimal threshold.

From examination of Fig. 1, it might be supposed that, by changing the activation function, one can improve signal detection performance. But this is not so. For any activation function f that satisfies our assumptions and any fixed input PDFs ρ_{X_S} and ρ_{X_A} , the unit’s performance at optimal threshold is the same. This is our constant optimal performance theorem (COPT); it is stated and proved in (11). In particular, for the logistic, increasing the gain G does not induce better performance. It may change the value of the threshold that yields optimal performance, but it does not change the actual performance at optimum. This is because a strictly increasing activation function gives a one-to-one mapping from input to output values. This makes it possible to express Eq. 2 exclusively in terms of the input PDFs ρ_{X_S} and ρ_{X_A} , and α , ω , and λ . Because it is the overlap between ρ_{X_S} and ρ_{X_A} that limits performance, and because this overlap does not vary with the gain, the performance at optimal threshold is constant.

We now examine the effect of changing the gain on the SNR of the output of a single unit. In electrical engineering, the SNR measures the difficulty of extracting a continuous-time signal $s(t)$ from a noisy background $n(t)$. The SNR compares the average power input to the receiver in the presence of the signal, $\mathcal{S} = \langle [s(t) + n(t)]^2 \rangle$, with the average power input in the absence of the signal, $\mathcal{N} = \langle n(t)^2 \rangle$ (12). If $s(t)$ is a small perturbation added to $n(t)$, then $\mathcal{S} \approx \mathcal{N}$, and the signal will be difficult to detect. On the other hand, if the signal amplitude is high and the noise amplitude is low, then $\mathcal{S} \gg \mathcal{N}$. Thus, the ratio \mathcal{S}/\mathcal{N} measures how difficult it is to distinguish signal from noise.

In the case of a single unit, if the unit’s input is x , its output is $y = f_G(x)$. Because

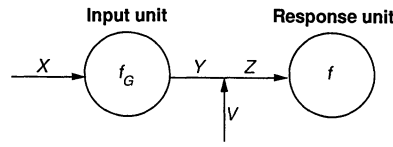


Fig. 2. A chain of units. The output of the unit receiving the signal is combined with noise to provide input to a second unit called the response unit. The activation of the response unit is compared with a threshold to determine the presence or absence of the signal.

this quantity represents the firing rate of the neuron for a given stimulus presentation, if each neural spike contains the same amount of energy, the power the neuron delivers will be proportional to γ . Thus, over many stimulus presentations, the average power delivered in the presence of signal is proportional to $\mu(Y_{GS})$, the mean of Y_{GS} , and in the absence of signal is proportional to $\mu(Y_{GA})$. Hence, the ratio of the average power delivered in the presence of the signal to the average power delivered in the absence of the signal, that is, the SNR, is $\mu(Y_{GS})/\mu(Y_{GA})$.

In general, raising G will drive up $\mu(Y_{GS})$ and drive down $\mu(Y_{GA})$, increasing the SNR of a single unit. Yet by the COPT, the performance of the unit at optimal threshold remains the same, because the effect of an increase of G on ρ_{Y_S} and ρ_{Y_A} is not captured by the mean alone. Increases in G will in general alter the shapes of these PDFs, possibly driving apart the main concentrations of probability mass but simultaneously extending their tails (Fig. 1C). The erroneous intuition that separating the means will improve performance arises from the assumption that the effect of an increase in G is to translate the output PDFs rigidly away from one another. For this reason, it is misleading to explain the performance effects of catecholamines solely in terms of the SNR.

Although increasing G does not affect the signal detection performance of a single element, it does improve the performance of a chain of such elements. By a chain, we mean an arrangement in which the output of the first unit provides the input to another unit. Let us call this second element the response unit. We monitor the output of this second unit to determine the presence or absence of a signal (Fig. 2).

As in the previous discussion, noise is added to the net input of each unit in the chain in the presence as well as in the absence of a signal (13). We represent noise as a random variable (RV) V , with PDF ρ_V that we assume to be independent of gain. Let the RVs X_S , X_A , Y_{GS} , Y_{GA} , and their PDFs all be defined as in the single-unit case. Now, because noise is added to the net input of the response unit as well, the input

of the response unit is the RV $Z_{GS} = Y_{GS} + V$ or $Z_{GA} = Y_{GA} + V$, again depending on whether the signal is present or absent. We write $\rho_{Z_{GS}}$ and $\rho_{Z_{GA}}$ for the PDFs of these RVs. Then $\rho_{Z_{GS}}$ is the convolution of $\rho_{Y_{GS}}$ and ρ_V , and $\rho_{Z_{GA}}$ is the convolution of $\rho_{Y_{GA}}$ and ρ_V . Convoluting the output PDFs of the input unit with the noise distribution increases the overlap between the resulting distributions ($\rho_{Z_{GS}}$ and $\rho_{Z_{GA}}$) and therefore decreases the discriminability of the input to the response unit.

How are these distributions affected by an increase in G on the input unit? By the COPT, we already know that the discriminability of Y_{GS} and Y_{GA} is unchanged. Furthermore, we have assumed that the noise distribution is independent of G . It would therefore seem that a change in G should not affect the discriminability of Z_{GS} and Z_{GA} . However, under very general conditions, the overlap between $\rho_{Z_{GS}}$ and $\rho_{Z_{GA}}$ decreases when the G of the input unit increases, thereby improving performance of the two-layered system. We call this the chain effect.

The chain effect arises because the noise added to the net input of the response unit is not affected by variations in G . Increasing G separates the means of the output PDFs of the input unit, $\mu(Y_{GS})$ and $\mu(Y_{GA})$, even though this does not affect the performance of this unit. Suppose all the probability mass were concentrated at these means. Then $\rho_{Z_{GS}}$ would be a copy of ρ_V centered at $\mu(Y_{GS})$, and $\rho_{Z_{GA}}$ would be a copy of ρ_V centered at $\mu(Y_{GA})$. Thus, in this case, increasing G would rigidly translate $\rho_{Z_{GS}}$ and $\rho_{Z_{GA}}$ apart, thereby reducing their overlap and improving performance. A similar effect arises in more general circumstances, when Y_{GS} and Y_{GA} are not concentrated at their means. The chain performance theorem, stated and proved in (11), gives sufficient conditions for the appearance of this effect.

The above analysis has shown that increasing the G of the activation function of individual units in a very simple network can improve signal detection performance. We now present computer simulation results showing that this phenomenon can account for catecholamine-induced performance improvements in a common behavioral test of signal detection.

The continuous performance test (CPT) (14) has been used extensively to study attention and vigilance in behavioral and clinical research. In this task, individual letters are displayed tachistoscopically in a sequence on a computer monitor. In one common version of the task, a target event is to be reported when two consecutive letters are identical. Performance on this task has been shown to be sensitive to drugs or

pathological conditions affecting catecholamine systems (15–17). During baseline performance, subjects typically fail to report 10 to 20% of targets (“misses”) and inappropriately report a target during 0.5 to 1% of the remaining events (“false alarms”). After the administration of agents that directly release catecholamines from synaptic terminals and block re-uptake from the synaptic cleft (CNS stimulants such as amphetamines or methylphenidate), the number of misses decreases while the number of false alarms remains approximately the same. Using standard measures of signal detection theory, investigators have shown that this pattern of results reflects an improvement in the discrimination between signal and nonsignal events (d'), whereas the response criterion (β) does not vary significantly (16, 17).

We used the backpropagation learning algorithm (18) to train a recurrent network of three layers (input layer, intermediate or hidden layer, and output layer) to perform the CPT (see Fig. 3A). In this model, several simplifying assumptions made in the preceding section are removed. First, the network contains recurrent connections. Second, connection weights are developed entirely by the training procedure; as a result, the activation patterns on the intermediate layer that are evoked by the presence or absence of a signal are also determined solely by the training procedure. Finally, the representation of the signal is distributed over an

ensemble of units rather than determined by a single unit.

After training, Gaussian noise with zero mean was added to the net input of each unit in the intermediate and output layers as each letter was presented. The overall standard deviation of the noise distribution and the threshold of the response unit were adjusted to approximate the performance of human subjects under baseline conditions [human subjects: 11.7% misses and 0.6% false alarms (16); simulation: 13.0% misses and 0.75% false alarms]. We then increased the G of all the intermediate and output units from 1.0 to 1.1 to simulate the effect of catecholamine release in the network. This manipulation resulted in rates of 6.6% misses and 0.78% false alarms [human subjects: 5.5% misses and 0.5% false alarms with methylphenidate (16); see Fig. 3B].

The enhancement of signal detection performance in the simulation is a robust effect. It appears when G is increased in the intermediate layer only, in the letter units only, or in both. Because of the recurrent connections between the letter units and the intermediate layer, the chain effect appears when G is increased over either or both of them. The impact of the chain effect is to reduce the distortion, due to internal noise, of the distributed representation on the layer receiving inputs from the layer where G is increased. The improvement takes place even when there is no noise added to the

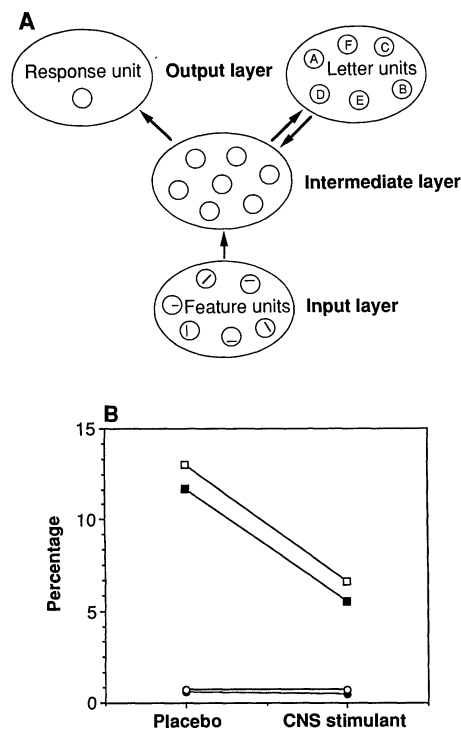
input of the response unit. The response unit in this network acts only as an indicator of the strength of the signal in the intermediate layer. Finally, as the COPT predicts, increasing G only on the response unit does not affect the performance of the network.

In this simulation, as well as in the preceding discussion, increasing G appears to have only the beneficial effect of making it easier to distinguish between the presence and absence of a signal. Nevertheless, it is possible to speculate about drawbacks of higher G values in a biological system. First, at lower G , the presence of noise guarantees some variability in response selection. Higher G may induce stereotyped responses. Variability of responses may be a necessary and adaptive feature of biological systems, particularly in the context of new environments and during learning.

Second, we have seen that increasing G reduces the effect of noise in a multilayer network. However, under some circumstances, what we have regarded as noise may be the expression of a weak signal that is competing with a stronger signal for transmission. In some situations, this weak signal may undergo progressive enhancement in subsequent layers of the network and ultimately be an important determinant of the system's response. With high values of G , the representation of this weaker signal would be eliminated early in processing, in favor of the stronger signal.

Finally, although operating at a high G improves signal detection performance, it may be energetically draining. Cortical neurons appear to operate at high G in states of wakefulness and arousal and at low G during sleep (19), and autoradiography studies suggest a correlation between catecholamine release and increased deoxyglucose metabolism (20). These observations are not surprising. The communication channels in the brain, like all communication pathways, have finite bandwidths, determined by their physical characteristics. The information capacity of such channels, operating in the presence of noise, is a function of the power emitted into them to transmit a signal (21). Hence, sending information over these channels at the rates associated with wakeful or alert behavior (that is, at higher G) requires higher power consumption or an increased rate of energy expenditure.

Fig. 3. Simulation of the continuous performance task. **(A)** Diagram of recurrent three-layer network (12 input units, 30 intermediate units, 10 output units, and 1 response unit). Each unit projects to all units in the subsequent layer. In addition, each output unit also projects to each unit in the intermediate layer. Letters are presented to the network as patterns of activation over the input units, which act as feature detectors. During training, the network learns to activate the output unit corresponding to the letter being presented on the input. In addition, the recurrent connections provide the network with the pattern of activation evoked on the output layer by the presentation of the previous letter. The network learns to activate the response unit when two consecutive letters are identical and to turn it off in all other cases. The activation of a unit in the intermediate or output layer depends on the activations of all units in the layers providing input to it. Each input is weighted by the corresponding connection strength, which can be positive or negative. The sum of the weighted inputs is then passed through the logistic function to determine the unit's activation. The gain parameter G is the same for all intermediate and output units. In the simulation of the placebo condition, $G = 1.0$; in the simulation of the drug condition, $G = 1.1$. Bias B is -1 in both conditions. **(B)** Performance of human subjects and of the simulation on the CPT. Filled markers indicate the performance of human subjects with placebo and methylphenidate (16). Empty markers indicate the results of the simulation.



REFERENCES AND NOTES

1. S. E. Loughlin, S. L. Foote, J. H. Fallon, *Brain Res. Bull.* **9**, 287 (1982); O. Lindvall and A. Bjorklund, *Neurol. Neurobiol. N.Y.* **10**, 9 (1984).
2. The effect of catecholamines on target cells is generally characterized as an enhancement of stimulus-elicited responses with respect to background firing

- rate. Some investigators have reported that this phenomenon arises simply from an inhibitory action of norepinephrine or dopamine on the cell, which depresses background firing rate more than it depresses stimulus elicited responses [for example, (5); E. T. Rolls, S. J. Thorpe, M. Boytim, I. Szabo, D. I. Perret, *Neuroscience* **12**, 1201 (1984)]. In this report, we focus on a set of observations that suggests a different mechanism: a potentiation of responses to both excitatory and inhibitory inputs with minimal or no influence on background firing rate [for example, (6, 7)]. Furthermore, in considering these changes in cellular response, we are not attempting to address the underlying biochemical mechanisms. Our focus, and our results, concern the informational and behavioral consequences of neuromodulation, at the cellular level and above.
3. S. L. Foote, *Annu. Rev. Neurosci.* **10**, 67 (1987).
 4. C. R. Clark, G. M. Geffen, L. B. Geffen, *Neurosci. Biobehav. Rev.* **11**, 353 (1987).
 5. S. L. Foote, R. Freedman, A. P. Olivier, *Brain Res.* **86**, 229 (1975).
 6. L. A. Chiodo and T. W. Berger, *ibid.* **375**, 198 (1986).
 7. D. J. Woodward, H. C. Moises, B. D. Waterhouse, B. J. Hoffer, R. Freedman, *Fed. Proc.* **38**, 2109 (1979).
 8. S. Sara, *Physiol. Psychol.* **13**, 151 (1985); S. L. Foote, F. E. Bloom, G. Aston-Jones, *Physiol. Rev.* **63**, 844 (1983); M. Segal, *Physiol. Psychol.* **13**, 172 (1985); R. D. Oades, *Neurosci. Biobehav. Rev.* **9**, 261 (1984); E. M. Stricker and M. J. Zigmond, in *Handbook of Physiology: Section 1, The Nervous System*, vol. 4: *Intrinsic Regulatory Systems of the Brain*, F. E. Bloom, Ed. (Oxford Univ. Press, New York, 1986), pp. 677-700; W. F. Hopkins and D. J. Johnston, *J. Neurophysiol.* **59**, 667 (1988); A. N. Mamelak and A. J. Hobson, *J. Cognit. Neurosci.* **1**, 201 (1989).
 9. G. E. Hinton and T. J. Sejnowski, in *Proceedings of the Fifth Annual Conference of the Cognitive Science Society* (Lawrence Erlbaum, Hillsdale, NJ, 1983); Y. Burnod and H. Korn, *Proc. Natl. Acad. Sci. U.S.A.* **86**, 352 (1989).
 10. The logistic is used purely as a familiar example. Our analysis applies to any suitable family of functions, $\{f_G\}$. We require only that each member function f_G is strictly increasing, and that, as $G \rightarrow \infty$, the family $\{f_G\}$ converges to the unit step function u_0 almost everywhere. Here, u_0 is defined as

$$u_0(x) = \begin{cases} 0 & \text{for } x \leq 0 \\ 1 & \text{for } x > 0 \end{cases}$$
 A sequence of functions $\{g_n\}$ converges almost everywhere to the function g if the set of points where it diverges, or converges to the wrong value, is of measure zero. For a rigorous discussion of convergence almost everywhere, consult A. J. Weir, *Lebesgue Integration and Measure* (Cambridge Univ. Press, Cambridge, 1973).
 11. H. Printz and D. Servan-Schreiber, "Foundations of a computational theory of catecholamine effects," *Technical Report CMU-CS-90-105* (Carnegie Mellon University School of Computer Science, Pittsburgh, PA, 1990).
 12. The angle brackets represent time-averaging. The quantities being averaged are the squares of the incident amplitudes, because these are proportional to the incident energy.
 13. In this discussion, we have assumed that the same noise was added to the net input of each unit of the chain. However, the performance improvement does not depend on this assumption.
 14. H. E. Rosvold, A. F. Mirsky, I. Sarason, E. D. Bransome, L. H. Beck, *J. Consult. Psychol.* **20**, 343 (1956).
 15. C. Kornetzky and M. H. Orzack, *Psychopharmacologia* **6**, 79 (1964); K. H. Nuechterlein, *Schizophr. Bull.* **10**, 160 (1984).
 16. L. J. Pelouquin and R. Klorman, *J. Abnorm. Psychol.* **95**, 88 (1986).
 17. J. Rapoport et al., *Arch. Gen. Psychiatry* **37**, 933 (1980); R. Klorman et al., *Psychopharmacol. Bull.* **20**, 3 (1984).
 18. D. E. Rumelhart, G. E. Hinton, R. J. Williams, *Nature* **323**, 533 (1986).
 19. G. Aston-Jones and F. E. Bloom, *J. Neurosci.* **1**, 876 (1981); M. Livingstone and D. Hubel, *Nature* **291**, 554 (1981).

20. J. McCulloch, *Handb. Psychopharm.* **15**, 321 (1982); J. McCulloch, H. E. Savaki, M. C. McCulloch, J. Jehle, L. Sokoloff, *Brain Res.* **243**, 67 (1982).
21. C. E. Shannon, *Proc. Inst. Radio Eng.* **37**, 10 (1949).
22. W. J. Freeman, *Biol. Cybern.* **33**, 243 (1979).
23. We thank J. L. McClelland, H. A. Simon, and the Santa Fé Institute for their assistance in the development of these ideas. This research was supported in part by a National Institute of Mental Health IF Award (MH09696); in part by the Defense Advanced Research Projects Agency (Department of Defense), monitored by the Space and Naval War-

fare Systems Command under contract N00039-87-C-0251, Advanced Research Project Agency order 4864; in part by a National Institute of Mental Health PS Award (MH00673); and in part by a Scottish Rite Schizophrenia Research Program award. The views and conclusions contained in this document are those of the authors and should not be interpreted as representing the official policies, either expressed or implied, of the Defense Advanced Research Project Agency or the U.S. government.

17 January 1990; accepted 31 May 1990

The C₇ Cluster: Structure and Infrared Frequencies

J. R. HEATH, R. A. SHEEKS, A. L. COOKSY, R. J. SAYKALLY

Observation and characterization of the C₇ cluster are reported. Carbon clusters are produced by laser vaporization of a graphite target followed by supersonic expansion of the vaporized material within a gas dynamically focused argon jet. Thirty-six sequential rovibrational lines of the ν_4 antisymmetric stretch fundamental of C₇ are probed by gated detection of diode laser absorption. The observed spectrum is characteristic of a symmetrical linear molecule. Analysis of the spectrum indicates an effective average bond length of 1.2736(4) angstroms and a vibrational frequency of 2138.1951(10) reciprocal centimeters, in excellent agreement with ab initio calculations. This work will facilitate the astrophysical detection of this cluster.

SMALL CARBON CLUSTERS (LESS THAN 12 atoms) have recently attracted the attention of numerous investigators from a wide variety of disciplines. This is largely due to the ubiquitous nature of these species; they have been observed in astrophysical sources (1), in sooting flames (2), in acetylene photolysis (3, 4), and in plasmas produced by laser vaporization of graphite (5-7). This suggests that unsaturated carbon clusters play a critical, if not central, role in the high-temperature chemistry of carbon-rich environments.

Ab initio and semiempirical theory of small carbon clusters has been under constant development for several decades (8, 9). Much of this work has recently been reviewed by Weltner and Van Zee (10). Odd-numbered clusters of up to 11 atoms are expected to have linear $^1\Sigma$ ground states, with the lowest triplet states existing at much higher energy. Even-numbered clusters of up to 10 atoms are predicted to have two low-energy configurations: an open shell linear $^3\Sigma$ state and a monocyclic singlet state. There is much debate regarding the detailed properties of these even clusters (10). Odd-numbered clusters up to C₇ are predicted to be more stable than the adjacent even clusters (9).

Despite this high level of theoretical activity, experimental results have been sparse. The development of tandem mass spectro-

metric technologies has enabled researchers to study carbon cluster cation photofragmentation (6) and anion photoelectron spectroscopy (7). Results from these experiments have been consistent with theory. Only recently, however, have definitive experiments capable of testing detailed theoretical predictions been possible. Over the past 2 years a number of research groups have characterized the C₃ cluster with high-precision laser techniques and have obtained sufficient information for the construction of an accurate molecular potential surface (3, 12-14). Last year we accomplished a detailed laboratory characterization of the C₅ cluster (5) using infrared laser spectroscopy. That experiment was reported simultaneously with the detection of C₅ in the carbon star IRC+10216 by Bernath, Hinkle, and Keady (1). Additional bands of C₅ have been detected and analyzed by Moazzen-Ahmadi, McKellar, and Amano (4, 15). Ab initio calculations are in close agreement with those experimental results.

In this paper we describe direct observation and characterization of the C₇ cluster, carried out with an infrared laser spectroscopy technique similar to that used in our study of C₅. Thirty-six sequential rovibrational lines have been measured and assigned to the ν_4 antisymmetric stretch vibrational transition of C₇. The observed spectrum is characteristic of a symmetrical linear molecule with a closed electronic shell. Analysis of the spectrum indicates a ground state rotational constant of 0.030929(21) cm⁻¹,

Department of Chemistry, University of California, Berkeley, CA 94720.